EFFECT OF HYBRID REINFORCEMENT ON CRACK INITIATION AND PROPAGATION MECHANISM IN METAL MATRIX COMPOSITES DURING LOW CYCLE FATIGUE

AKM Asif Iqbal[1*], Yoshio Arai[2], Wakako Araki[3]

[1]*Graduate School of Science and Engineering, Saitama University, 255 Shimo-okubo, Sakura-ku, Shaitama city 338-8570, Japan*
[2,3]*Department of Mechanical Engineering, Saitama University, 255 Shimo-okubo, Sakura-ku, Shaitama city 338-8570, Japan*
**partho229@yahoo.com*

Keywords: Metal matrix composites (MMCs), Microcrack initiation, Microrack propagation, Low cycle fatigue

Abstract
Microcrack initiation and propagation mechanism during low cycle fatigue were studied in three types of materials; Hybrid MMC, MMC with Al_2O_3 whiskers and Al alloy and the role of hybrid reinforcement was examined. The microcracks initiated at the boundary between Si particles cluster and Al grain in case of Al alloy but the initiation location changed to the interface of whisker-matrix and particle-matrix when reinforcements were added to the matrix. Moreover, microcracks initiated very early in the fatigue life of hybrid MMC compare to other two materials. Besides, interface debonding followed by void nucleation dominates the fracture of MMCs whereas fracture occurs in Al alloy due to the formation of voids and plastic slip.

1 Introduction

The development of metal matrix composites (MMCs) has set the stage for a new revolution in materials. Among the different types of MMCs, aluminium matrix composites reinforced with discontinuous reinforcements have generated significant interest as they provide best combination of strength, ductility and toughness and can be manufactured by conventional processing techniques [1].

Though MMCs have many advantages, problems still remain with their poor damage tolerance properties under monotonic or cyclic loads [2]. Many applications for which MMC materials are used involve cyclic loading, and therefore, fatigue properties are of critical interest. The fatigue life of a component depends on the initiation and growth of a crack which finally caused failure [3]. However, the exact role of the reinforcement phase in fatigue crack initiation and growth processes is not well understood. Chawla et al.[4] found 10 μm length microcracks early in the fatigue life at the particle matrix interface while studying 2080 Al/ SiCp composite. Chen et al. [1] found higher density of microcracks within 100μm range while studying 2124 Al-20 vol% SiCw composite. These microcracks rapidly initiated at 10% of total life in reinforcement/matrix interface, grew quickly and coalesced to form a dominant crack which leads to specimen failure. While fatigue crack initiation in MMC represents a significant fraction of the total fatigue life, fatigue crack growth stage can also be important.

The crack growth behavior in particle reinforced MMCs are very much dependent on reinforcement characteristics and on matrix microstructure. In general, crack propagation thresholds are higher for composites than for their matrices alone [5]. Besides, the fracture mechanism of hybrid MMC under monotonic and cyclic load was investigated by Rafiquzzaman et. al.[6]. They observed fracture surfaces and concluded that fracture of hybrid MMC under cyclic load was dominated by the interfacial debonding of particle/matrix and whisker/matrix interfaces. The results of microcrack initiation and propagation, referenced earlier, weigh in favor of either particulate reinforced or whisker reinforced MMCs. So far the research of hybrid MMCs are limited in the investigation of fracture mechanism and wear properties [7]. Studies of the effect of hybrid reinforcement on microcrack initiation and propagation mechanism are rare. The present study investigated the initiation, interaction and coalescence of fatigue microcracks in smooth specimens of three different types of materials and described the effect of hybrid reinforcement on fatigue crack initiation and propagation mechanism in low cycle fatigue.

2 Materials and experimental procedures

Three types of materials were used to investigate the crack initiation and propagation mechanism. Aluminium alloy JIS-AC4CH [8], metal matrix composite with 9 vol% Al_2O_3 whiskers as reinforcement and hybrid metal matrix composite with 21 vol% SiC particles and 9 vol% Al_2O_3 whiskers as reinforcements. The chemical composition of AC4CH alloy is listed in Table 1. The volume fractions and mechanical properties of hybrid MMC and MMC with Al_2O_3 whiskers are shown in Table 2. All the specimens used in this study were rectangular shape with the dimension of 100x8x6 mm length, width and height respectively.

Si	Fe	Mg	Ti	Al
7.99	0.2 (max.)	0.57	0.07	Bal.

Table 1. Chemical composition of AC4CH alloy, wt%

Parameters	Al_2O_3	SiC	Al alloy AC4CH	Hybrid MMC	MMC with Al_2O_3
Young's modulus (GPa)	380	450	70.0	142	104
Poisson's ratio	0.27	0.20	0.33	0.28	0.29
Yield strength (MPa)	-	-	131	166	141
Tensile strength (MPa)	-	-	262	228	200

Table 2. Volume fraction and mechanical properties

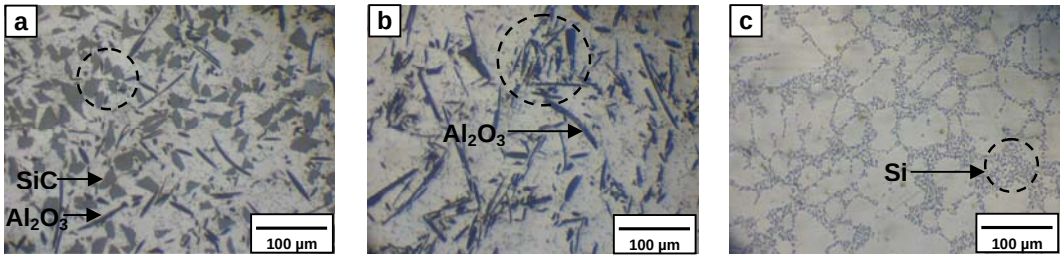

Figure 1. Microstructure of (a) Hybrid MMC, (b) MMC with Al_2O_3 whiskers and (c) Al alloy

The machined surface of the specimens were polished using polishing machine. The microstructures of three types of materials are shown in Fig.1. The SiC particles in hybrid MMC are rectangular shaped with sharp corners and the Al_2O_3 whiskers for both hybrid MMC and MMC with Al_2O_3 are roller shaped as shown in Fig.1a and 1b. The SiC particles have an average length of 23 µm. The average length and average diameter of the Al_2O_3

whiskers are 33 µm and 2 µm respectively. In Al alloy, Al has an average grain size of 48 µm. The Si particles in Al alloy are round shaped with an average diameter of 3 µm. At frequent intervals a clustering of SiC particles and Al_2O_3 whiskers was observed in hybrid MMC and MMC with Al_2O_3 as shown by the broken lines in Fig. 1a and 1b respectively. Clustering of Si is also observed in the Al alloy as shown by the broken line in Fig.1c.Three point bending tests were performed in a Shimazu servopulser machine. Monotonic bending tests were conducted with a displacement rate of 0.0025 mm s^{-1}. Strength of three different materials was calculated from the maximum load at failure as a nominal bend stress σ_c. Cyclic fatigue tests were conducted in the load control mode under the load ratio R = 0.1 at the frequency of 0.5 Hz. Three tests of each material were conducted with the maximum stress of $0.7\sigma_c$, $0.8\sigma_c$, and $0.9\sigma_c$. All tests were carried out at room temperature. The number of cycles to failure is taken as the fatigue life N_f. The plastic replica technique was used to study the initiation and growth of microcracks at various times during the fatigue life. The tensile surfaces and the fracture surfaces were comprehensively examined in a Scanning Electron Microscope (SEM) and Energy-dispersive x-ray spectroscopy (EDS) to determine the crack initiation site.

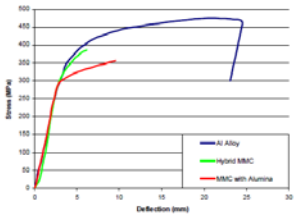

Figure 2. Nominal bending stress Vs deflection curves

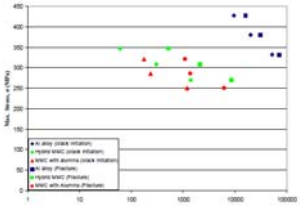

Figure 3. S-N diagram

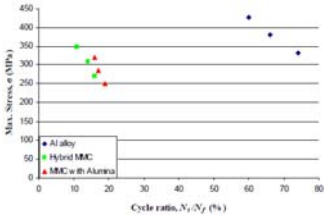

Figure 4. Microcrack Initiation at different stress and cycle ratio

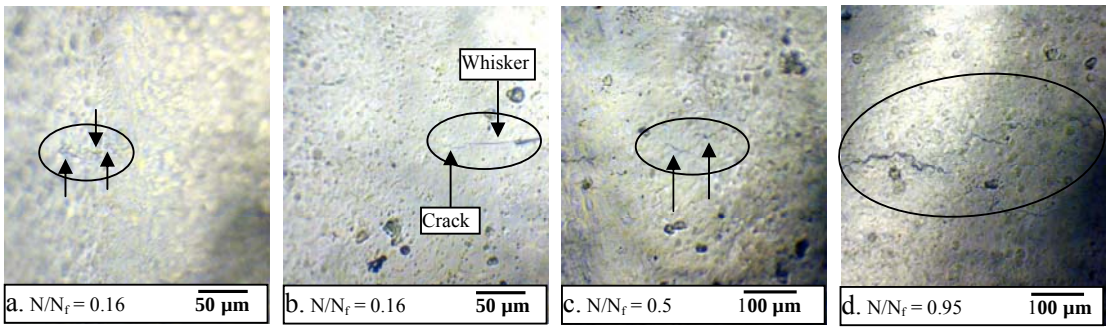

Figure 5. Crack initiation and propagation at various stages of fatigue life of hybrid MMC: σ_c = 270 MPa, N_f = 8580 cycles

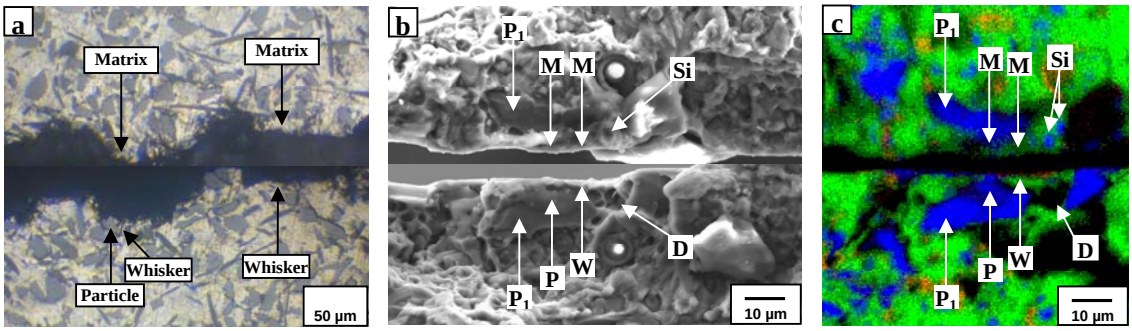

Figure 6. Crack initiation site at the matching surface of the fractured specimen (a) optical micrograph, (b) SEM micrograph, (c) EDS analysis: hybrid MMC, σ_c = 270 MPa

3 Experimental results and discussion

3.1 Monotonic test

The nominal bending stress and deflection curves measured by the three point bending test are presented in Fig 2. The hybrid MMC and MMC with Al_2O_3 whisker were fractured at 386 and 357 MPa respectively but the Al alloy did not fracture rather it was plastically collapsed at 475 MPa. The fatigue test was conducted based on the fracture stress of these three materials. The collapsed stress of Al alloy was used as the fracture stress during fatigue test.

3.2 Fatigue test

Fig. 3 shows the number of cycles to initiate microcracks, N_i, and final failure, N_f, at different stress levels of hybrid MMC, MMC with Al_2O_3 whiskers and unreinforced Al alloy and Fig. 4 represents microcrack initiation at different cycle ratio N_i/N_f of those materials. The crack initiation life and the total fatigue life of hybrid MMC are superior to that of MMC with Al_2O_3 whiskers in low cycle fatigue which is exhibited in Fig. 3. In hybrid MMC, microcracks were initiated very early in the fatigue life. For example, in case of 0.7 σ_c stress level, microcracks initiated only at 1400 cycles (Fig. 3) which is 16% (Fig. 4) of the fatigue life. For the same stress level, microcracks initiated at 1200 cycles (Fig. 3), 19 % (Fig. 4) of the fatigue life in MMC with Al_2O_3 whiskers and 52000 cycles (Fig. 3), 74 % (Fig. 4) of the fatigue life in case of unreinforced Al alloy. Therefore, it is well understood that, the propagation life in cycle ratio for hybrid MMC is very long compare to that of other two materials.

3.3 Microcrack initiation and propagation

3.3.1 Hybrid MMC

The evolution of fatigue microcracks on the surface of the materials can be followed from optical micrograph observation at the same areas on replicas. The optical micrographs of replicas obtained at various stages of fatigue testing of hybrid MMC at 0.7 σ_c = 270 MPa peak stress are shown in Fig. 5. At 16% of fatigue life, several cracks were initiated (Fig. 5a). Another crack at the same time initiated at a region next to the edge of an Al_2O_3 whisker (Fig. 5b). These cracks were initiated with the size of 15-20 μm. Due to the continued cycling of fatigue these cracks coalesced each other and their lengths were increased. At 50% of the fatigue life, few cracks of length between 25 to 50 μm were formed in between these two main cracks initiated earlier (Fig. 5c). At 95% of the fatigue life all these cracks coalesced to each other and a fatal crack was produced (Fig. 5d). The size of the fatal crack was around 650 μm on the specimen surface. The final failure took place at 8580 cycles. Similar microcrack initiation and coalescence phenomena were observed in the test under other maximum stresses. Fig. 6a represents the optical micrograph of crack initiation site where microcracks are found initiated at particle/ matrix interface. An Al_2O_3 whisker was also found located very close to the crack initiated SiC particle (Fig. 6a). Fig. 6b represents the SEM micrograph of microcrack initiation site at the cluster of SiC particles and Fig. 6c shows the EDS mapping analysis on the areas corresponding to Fig. 6b. The green, blue and red color in Fig. 6c represents the presence of Al, Si and O respectively on the fracture surfaces. In Fig 6c, the blue colored area indicated by P contains a lot of Si (96%) and a small amount of Al (4%) which means the area is SiC particle and the green colored area indicated by left M contains a lot of Al (93%) and a small mount of Si (7%) which means the area is Al matrix. Therefore, the blue and green colored area indicated by P-M pair (corresponding to P-M pair of Fig. 6b) denoted the crack initiation site (Fig. 5a) where SiC particle/matrix interfacial debonding occurred. The P_1- P_1 pair in Fig. 6b and 6c indicates the presence of SiC particles on both side of the fractured surface, means the interface debonding was followed by the transgranular fracture in this crack initiation site. The area where green and red colors exist together indicates the presence of Al and O together means the area is Al_2O_3 whisker denoted by W in Fig. 6c. This Al_2O_3 whisker was found exist very close to the debonded SiC particle.

Interfacial debonding was also found being occurred in this Al_2O_3 whisker which is indicated by W-M pair in Fig. 6c (corresponding W-M pair in Fig 6b). Besides, lot of dimples were found nucleated (arrow 'D' in Fig. 6b) in aluminium alloy matrix. The EDS mapping analysis confirms the presence of few Si particles on the opposite side of the dimples (arrow 'Si' in Fig. 6c) indicating void nucleation is induced by the plastic deformation concentration of Al matrix at the second phase Si particles. Hence, the fracture mechanism of hybrid MMC during cyclic loading is dominated by the particle/ matrix and whisker/matrix interfacial debonding as well as transgranular fracture followed by void nucleation in Al alloy matrix.

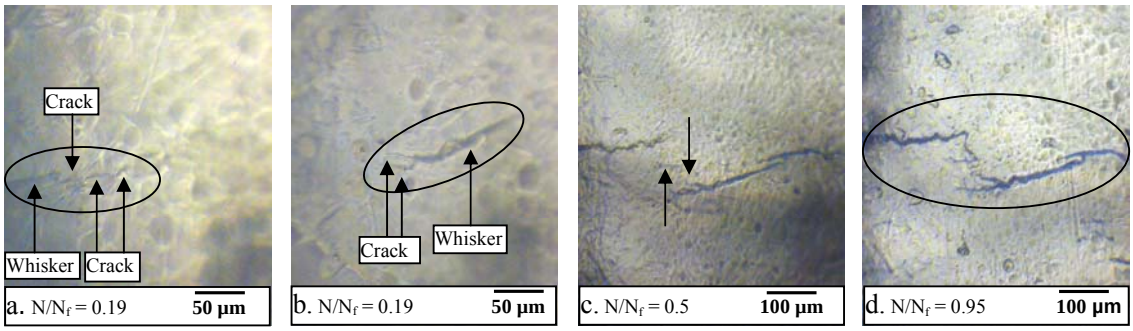

Figure 7. Crack initiation and propagation at various stage of fatigue life of MMC with Al_2O_3 whiskers: σ_c = 250 MPa, N_f = 6200 cycles

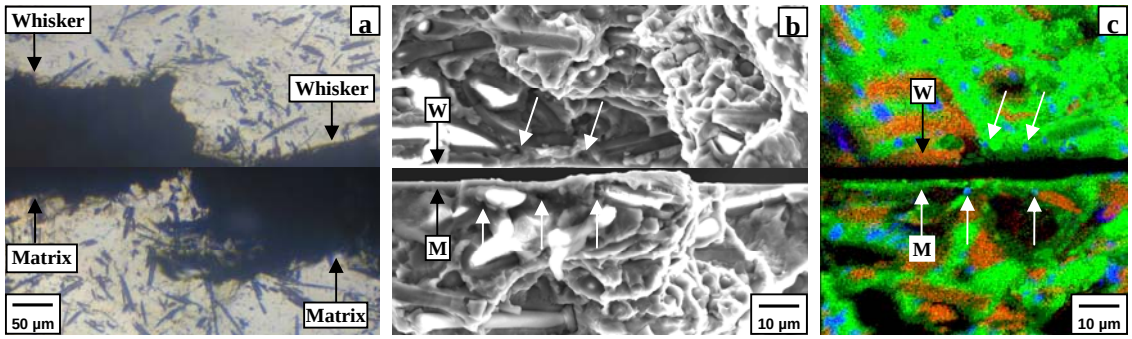

Figure 8. Crack initiation site at the matching surface of the fractured specimen (a) optical micrograph, (b) SEM micrograph, (c) EDS analysis: MMC with Al_2O_3 whisker, σ_c = 250 MPa

3.3.2 MMC with Al_2O_3 whisker

Fig. 7 exhibits the optical micrographs of replicas obtained at various stages of fatigue testing of MMC with Al_2O_3 whiskers at 0.7 σ_c = 250 MPa peak stress. At 19% of fatigue life (Fig. 4), several cracks of lengths around 20-25 µm were found initiated at a region next to the edge of two whiskers (Fig. 7a and 7b). These cracks grew by their own in the Al alloy matrix and their lengths were increased due to continued fatigue cycling. Besides, at 50% of the fatigue life few cracks of length below 25 µm were found initiated at a region next to the edge of a whisker in between these two main cracks (Fig. 7c). At 95% of the fatigue life, all these cracks coalesced to each other as shown in Fig. 7d. Thickness of both the whiskers where microcracks originally initiated was found increased means the whiskers along the line of the cracks were debonded. The fatal crack was produced joining both debonded whiskers. The size of the fatal crack was around 825 µm. The final failure took place at 6200 cycles. The phenomena of microcrack initiation and coalescence were found quite similar in the test under other higher stresses. Fig. 8a exhibits the optical micrograph of crack initiation site at the matching tensile surface of fractured specimen. It is seen that microcracks initiated at the edge of two whisker/matrix interface. Fig. 8b represents the SEM micrograph of microcrack initiation site and Fig. 8c shows the EDS mapping analysis on the areas corresponding to Fig.

8b. The presence of Al, Si and O on fracture surface is represented by the green, blue and red color respectively. In Fig. 8c, the red colored area indicated by W contains Al (82%) and O (18%) which means the area is Al_2O_3 whisker and the green colored area M contains Al (94%) and Si (6%) indicating the area is Al matrix. Therefore, the red and green colored area indicated by W-M pair in the matching halves denoted Al_2O_3 whisker/matrix interfacial debonding where the crack initiation occurred next to the whisker (corresponding W-M pair in Fig 8b). Few dimples were originated at the crack initiation site (arrows in Fig. 8b) in Al alloy matrix. The EDS analysis shows the presence of Si particle on the opposite side of the dimple like shape (blue colored points indicated by arrows in Fig. 8c) which means the void nucleation is induced by the plastic deformation concentration at the Si particle. Therefore, the fracture mechanism of MMC with Al_2O_3 whisker is directed by the whisker-matrix interfacial debonding followed by the void nucleation in Al alloy matrix.

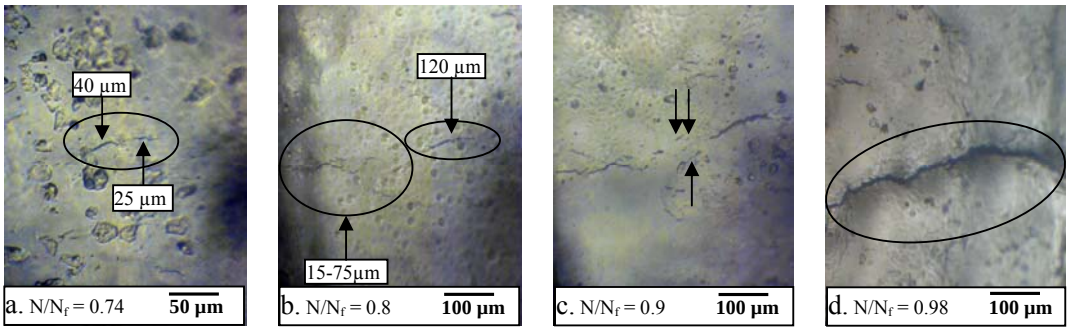

Figure 9. Crack initiation and propagation at various stages of fatigue life of Al alloy : σ_c = 332 MPa, N_f = 70000 cycles

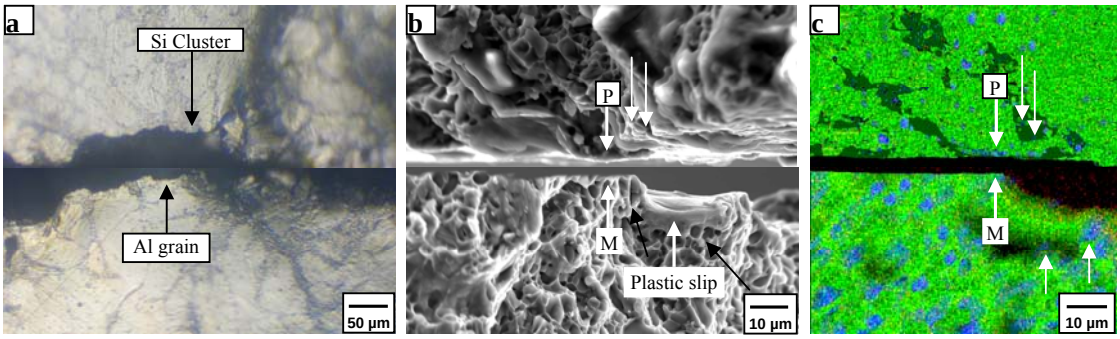

Figure 10. Crack initiation site at the matching surface of the fractured specimen (a) optical micrograph, (b)SEM micrograph, (c) EDS analysis: Al alloy, σ_c = 332 MPa

3.3.3 Al alloy

Fig. 9 shows the crack initiation and propagation at various stages of fatigue life of Al alloy at $0.7\sigma_c$ = 332 MPa peak stress. In case of Al alloy, two cracks of lengths 25 and 40 µm were initiated at 74% of the fatigue life (Fig. 9a). At 80% of the fatigue life, these two cracks joined together and the length became 120 µm (Fig. 9b). At this stage many cracks of length between 15-75 µm were found initiated (Fig. 9b). These cracks grew by their own and coalesced with other nearby microcracks produced due to continued cycling. At 90% of the fatigue life, few other microcracks of length below 25 µm were found initiated between these cracks (arrows in Fig. 9c). At 98% life the fatal crack was produced joining all the cracks and the crack length was 1250 µm (Fig. 9d). Similar microcrack initiation and coalescence phenomena were exhibited in the tests under other maximum stresses. The optical micrograph of crack initiation site at the matching tensile surface of fractured specimen is shown in Fig. 10a.

Microcracks were found initiated between the boundary of Si particle cluster and Al grain. Fig. 10b shows SEM micrograph of the crack initiation site and Fig. 10c shows the EDS mapping analysis on the areas corresponding to Fig. 10b. In Fig 10c, the blue colored area indicated by P contains a lot of Si (98%) which means the area is Si particle and the green colored area indicated by M contains a lot of Al (97%) which means the area is Al grain. Therefore, the blue and green colored area indicated by P-M pair in the matching halves denoted the crack initiation site where Si particle/Al grain interfacial separation occurred (corresponding to the P-M pair in Fig. 10b). Plenty of dimples were nucleated around the P-M pair (indicated by arrows in Fig. 10b) in Al grain. Plastic slip like morphologies were also formed along the specimen surface (indicated in Fig. 10b). The EDS mapping analysis confirms the presence of few Si particles in the dimples (arrow in Fig. 10c) which means the void nucleation is induced by the plastic deformation concentration of Al matrix at the second phase Si particles. Moreover, the above observation clarifies that the fatigue fracture mechanism of Al alloy is directed by the interfacial debonding between Si particle and Al grain followed by void nucleation and formation of plastic slip due to high plastic deformation in aluminium grain.

3.4 Discussion

From the above results, it is found that in the unreinforced Al alloy cracks usually initiated at the boundary between Si particle cluster and Al grain. The crack initiation sites of MMC with Al_2O_3 whiskers were the region next to the edge of the whisker. On the contrary, in case of hybrid reinforcement the crack initiation sites were the interface of SiC particle and matrix and the region next to the edge of the Al_2O_3 whisker suggesting that interface debonding between SiC particles near the Al_2O_3 whisker and the matrix is a main feature of crack initiation. During cyclic loading, the reinforcing particles and whiskers are deforming elastically within the plastically deforming matrix alloy in low cycle fatigue. The plastic strain in the composite matrix between reinforcing particle and whisker is higher in hybrid MMC because the reinforcements do not experience plastic deformation. In addition, the stiff ceramic reinforcements act as stress concentrators, localizing the plastic strain between the particle and the whisker. Thus, large strain mismatch occurs between these two reinforcement materials and the Al alloy and stress concentration becomes high on the interface. Therefore, microcracks initiation resistance in hybrid MMC decreased and the cracks initiated at the interface of particle/whisker and Al alloy matrix. It is also observed that microcracks initiated very early at only 11% to 16% of the fatigue life in hybrid MMC (Fig. 4) with applied stress conditions whereas crack initiation delayed slightly in MMC with Al_2O_3 whisker and largely in Al alloy (Fig. 4). Moreover, it is noticed that once a whisker was very close to the cluster of SiC particle in hybrid MMC, crack initiation occurred in both particle/matrix and whisker/matrix interfaces (Fig. 5a and b) but the whisker which was far away from the particle did not have any contribution to initiate crack. During the loading and unloading process in cyclic deformation, cyclic hardening occurs due to the accumulation of plastic strain at the interface between matrix and reinforcement. Due to the presence of three different materials in very close vicinity, elastic plastic strain mismatch becomes very high and crack initiates early at that place. Therefore, due to the hybridization effect crack initiates early in hybrid MMC.

However, from replica observation it is found that microcracks propagated for a relatively long time after initiation to become a fatal crack and caused failure in hybrid MMC whereas relative crack propagation life was short in Al alloy. In case of Al alloy, microcracks grew smoothly through the boundary between Si particles cluster and Al grain without any noticeable resistance as shown in Fig.10a. Besides, in MMC with Al_2O_3, due to the random orientation of the whiskers, when a crack met a perpendicular whisker, whisker fracture ahead of the crack tip occurred. When it met a parallel whisker, interfacial separation occurred. As a result these cracks also propagated smoothly without any remarkable resistance and finally

caused failure (Fig. 8). On contrary, the crack had a tendency to avoid and detours round the particle in hybrid MMC (Fig. 6). In addition, no SiC particle was found broken at the surface of hybrid MMC indicating the strain localization was not high enough which could fracture the particle. However, greater strain mismatch could occur between particle and matrix and therefore interfacial separation took place. Consequently, the presence of stiff ceramic particles acted as a barrier to propagate crack smoothly and crack propagation was delayed in hybrid MMC.

4 Conclusions

This research concentrated to find out the crack initiation cycle and the crack initiation location as well as the behavior of crack propagation. The following conclusions have been reached in this study:

1. The addition of reinforcement changed the crack initiation site. In Al alloy, cracks initiated at the boundary between Si particles cluster and Al grain. In hybrid MMC and MMC with Al_2O_3 whiskers, cracks initiated at the particle matrix and whisker matrix interface respectively.
2. Cracks initiated very early of the fatigue life in hybrid MMC compared to other two materials indicating the reduction of crack initiation resistance due to the hybrid effect.
3. The crack propagation life of hybrid MMC is long compare to MMC with Al_2O_3 whiskers and Al alloy. The fracture mechanism of hybrid MMC and MMC with Al_2O_3 whiskers is dominated by the interface debonding of particle/ matrix and whisker/matrix followed by the void nucleation in Al alloy matrix whereas the fracture in Al alloy is directed by the interfacial separation of Si particle and Al grain followed by void nucleation and formation of plastic slip in aluminium.
4. The fatigue strength of hybrid MMC is reasonably higher than that of MMC with Al_2O_3 whiskers.

References

[1] E.Y. Chen, L. Lawson, M. Meshii. The effect of fatigue microcracks on rapid catastrophic failure in Al-SiC composites. Material Science and Engineering A 200, 192-206 (1995).

[2] N. Chawla , V.V. Ganesh. Fatigue crack growth of SiC particle reinforced metal matrix composites. International Journal of Fatigue, vol. 32, pp.856–863 (2010).

[3] Z.Z Chen, K. Tokaji. Effects of particle size on fatigue crack initiation and small crack growth in SiC particulate-reinforced aluminium alloy composites. Materials Letters 58, 2314-2321 (2004).

[4] N.Chawla, C. Andres, J.W.Jones, J.E. Allison. Effect of SiC volume fraction and particle size on the fatigue resistance of a 2080 Al/SiCp composite. Metallurgical and Materials Transactions A, Vol 29 A (1998).

[5] J.J. Bonnen, C.P. You, J.E. Allison, J.W. Jones: in Fatigue 90, H. Kitagawa and T. Tanaka, eds., MCE Publishing, Birmingham, United Kingdom, pp. 887-92 (1990).

[6] Md. Rafiquzzaman, Y. Arai, E. Tsuchida. Fracture mechanism of aluminium cast alloy locally reinforced by SiC particles and Al_2O_3 whiskers under monotonic and cyclic load. Materials Science and Technology; vol. 24 (3), pp. 273-280 (2008).

[7] Hui-Hui Fu, Kyung-seop han, Jung-II Song. Wear properties of saffil/Al, saffil/Al_2O_3/Al and saffil/SiC/Al hybrid metal matrix composites. Wear 256, 705-713 (2004).

[8] Aluminium alloy castings, JIS H5202, Japan Industrial Standard (2002)